

Leaching-Free Supported Gold Nanoparticles catalyzing Cycloisomerizations under Microflow Conditions

Felix Schröder^a, Nico Erdmann^b, Timothy Noël^{*b,c}, Rafael Luque^d and Erik V. Van der Eycken^{*a}

^a F. Schröder, Prof. Dr. E. V. Van der Eycken, Department of Chemistry, University of Leuven (KU Leuven), Celestijnenlaan 200F, B-3001 Leuven, Belgium. E-mail: Erik.VanderEycken@chem.kuleuven.be

^b Dr. N. Erdmann, Prof. Dr. T. Noël, Department of Chemical Engineering and Chemistry, Technische Universiteit Eindhoven, Den Dolech 2, 5600 MB Eindhoven, Netherlands. E-mail: t.noel@tue.nl

^c Prof. Dr. T. Noël, Department of Organic Chemistry, Ghent University, Krijgslaan 281 (S4), 9000 Ghent, Belgium.

^d Prof. Dr. R. Luque, Departamento de Química Organica, Campus de Rabanales, Edificio C-3 (Marie Curie – Anexo), Carretera Nacional IV – A, Km. 396, 14014 Córdoba, Spain.

Received: ((will be filled in by the editorial staff))



Supporting information for this article is available on the WWW under <http://dx.doi.org/10.1002/adsc.201#####>. (Please delete if not appropriate)

Abstract. A continuous-flow protocol for the gold-catalyzed cycloisomerization of sterically hindered Ugi-adducts to spiroindolines in a packed-bed reactor is presented. Spiroindolines with various substitution patterns are formed in good yields and with good selectivity.

A detailed characterization of the catalyst deactivation process was conducted, whereas no metal leaching from the catalyst was detected.

Keywords: gold nanoparticles, cycloisomerization, green chemistry, flow chemistry, heterogeneous catalysis

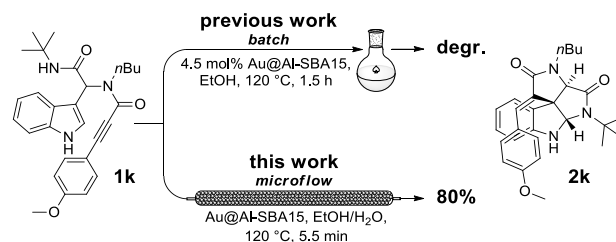
Introduction

Gold catalysis utilizing supported gold nanoparticles is an emerging topic in the intensively studied domain of gold-catalyzed reactions.^[1] Under homogeneous catalytic conditions, gold catalysis enables complimentary and unique reactivity to established synthetic transformations and allows one to work under mild reaction conditions. Notably, the rapid formation of complex biologically active structures via cycloisomerizations and C–C bond formations has experienced a boost by these developments.^[2] Supported gold nanoparticles combine the advantageous features of homo- and heterogeneous catalysis by merging the selective activation of π -systems with an uncomplicated recycling of the catalyst. Therefore, they provide opportunities to facilitate the application of gold catalysis on a larger scale. Nonetheless, in order to allow an application on an industrial scale, gold-catalyzed processes must be improved with regard to cost, productivity, robustness and environmental sustainability. A logical solution to overcome such issues is the use of a continuous-flow process utilizing highly active supported gold nanoparticles in a packed-bed reactor.^[3]

Several recent studies on the application of heterogeneous gold catalysts demonstrate the ability of such catalysts to be reused, which increases the sustainability of the overall reaction protocol.^[1,4] Although these catalytic systems require higher

temperatures than their homogeneous counterparts, they are more robust and do not require expensive ligands as well as sensitive activating reagents, such as hygroscopic silver salts (e.g. AgBF₄, AgNTf₂ and AgSbF₆). The latter avoids the potential occurrence of a silver effect.^[4-5]

The combination of heterogeneous gold catalysis with micro reactor technology offers various advantages compared to batch processes.^[6] Besides apparent benefits such as enhanced mixing, improved heat transfer, and safer reaction conditions, the use of a packed-bed reactor can increase selectivity and facilitate challenging transformations.^[3a,3c-g,7] Under continuous-flow conditions, usually short residence times are observed due to the increased amount of catalyst/reactant in the packed bed, resulting in less degradation of sensitive substrates, which can be seen in Scheme 1.



Scheme 1. Comparison of the gold-catalyzed spirocyclization of challenging Ugi-adducts in batch and continuous-flow with a packed-bed reactor.

Moreover, the use of a catalyst bed facilitates catalyst recycling and reuse, thereby reducing the amount of metal impurities in the final product.^[8]

Recently, our group developed a novel heterogeneous gold catalyst, consisting of gold nanoparticles on an Al-SBA15 support, for the cycloisomerization of Ugi-adducts.^[9] The reaction enabled access to various spiroindolines and diazepino[1,2-*b*]indazoles. A major advantage of the protocol was the use of ethanol as a sustainable solvent in substitution for dichloromethane or other chlorinated solvents, which are common for most gold-catalyzed reactions.^[11] The scope of the reaction was limited with regard to the substitution pattern of the alkynes within the Ugi-adducts. More specifically, an internal alkyne bearing methyl, ethyl or *para*-methoxyphenyl groups, resulted in prolonged reaction times under batch conditions, typically using catalyst loadings of 10 mol% at 80 °C. In many cases, the reaction did not proceed at all or only degradation of the starting material was detected. These problems were not encountered under homogeneous conditions using Au(PPh₃)SbF₆.^[10]

As part of our continuous effort to make gold catalysis more applicable on a large scale, we developed a continuous-flow process for the gold-catalyzed spirocyclization of Ugi-adducts employing supported gold nanoparticles in a packed-bed microreactor. In terms of reactivity, selectivity and productivity, the reported protocol proves to be superior to previous reports as shown in Scheme 1. The main reason for the superiority is the very high catalyst to substrate ratio in the packed-bed reactor.


Results and Discussion

The heterogeneous gold catalyst Au@Al-SBA15 was prepared via a ball-milling process.^[11] The mechanochemical method ensures that a large amount of the Au nanoparticles is deposited on the surface of the support and not inside the pores of the material. This feature avoids the need for molecular diffusion inside the particle and thus increases the catalytic activity of the nanocatalyst.^[12] An additional advantage of this process is the narrow diameter range of the nanoparticles and the homogeneous dispersion of the particles on the support surface.

The reaction was performed in a stainless steel packed-bed microreactor filled with Au@Al-SBA15 (see *Supporting Information* for details on the microfluidic setup).^[13] In an initial attempt, only traces of the desired product were observed at 80 °C and a residence time of 0.3 min (Table 1, Entry 1). By using hexafluoroisopropanol (HFIP) as an acidic additive, and slightly adjusting the flow conditions, full conversion could be achieved (Table 1, Entries 2-4). Control experiments demonstrated that the use of HFIP as a proton shuttle was mandatory to obtain full conversion (Table 1, Entries 5-7); even prolonged residence/reaction times did not lead to a complete consumption of the starting material in the absence of HFIP. Interestingly, the addition of 0.1 wt% water as a

cheap and sustainable proton shuttle resulted in an increase of reaction rate comparable to HFIP (Table 1, Entries 8 and 9). Optimal reaction conditions required a reduction of the flow rate to 15 μl/min and allowed for more demanding substrates to be efficiently converted (Table 1, Entry 10).

Table 1. Optimization of the reaction conditions for the gold-catalyzed cyclization of Ugi adducts using Au@Al-SBA15.^{a)}

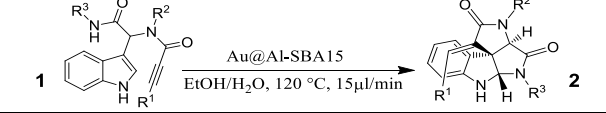


| Entry | Cat. [mg] | Temp. [°C] | Solvent | Flow [μl/min] | Reactor Volume [μl] | Res. Time [min] | Conv. [%] ^{c)} |
|-------|-----------|------------|-------------------------------------|---------------|---------------------|-----------------|-------------------------|
| 1 | 18 | 80 | 1-PrOH | 50 | 15 | 0.3 | < 10 |
| 2 | 24 | 100 | 1-PrOH/HFIP ^{b)} | 50 | 20 | 0.4 | 62 |
| 3 | 24 | 110 | 1-PrOH/HFIP ^{b)} | 25 | 20 | 0.8 | 74 |
| 4 | 24 | 120 | 1-PrOH/HFIP ^{b)} | 20 | 20 | 1.0 | 100 |
| 5 | 35 | 120 | 1-PrOH | 20 | 30 | 1.5 | 84 |
| 6 | 35 | 120 | 1-PrOH | 15 | 30 | 1.9 | 87 |
| 7 | 65 | 120 | 1-PrOH | 15 | 54 | 3.6 | 90 |
| 8 | 65 | 120 | EtOH | 15 | 54 | 3.6 | 90 |
| 9 | 75 | 120 | EtOH/H ₂ O ^{b)} | 15 | 62 | 4.1 | 100 |
| 10 | 75 | 120 | EtOH/H ₂ O ^{b)} | 25 | 62 | 2.5 | 72 |
| 11 | 100 | 120 | EtOH/H ₂ O ^{b)} | 15 | 83 | 5.5 | 100 |

^{a)} Experiments were performed with 25 mg of 1a in 0.8 ml of solvent; ^{b)} 0.1 wt% additive (i.e. HFIP or H₂O) used; ^{c)} conversion was determined by NMR.

With the optimal flow conditions in hand, the scope of the reaction was determined and the results are shown in Table 2.

Table 2. Scope of the Au catalyzed cyclization in flow.

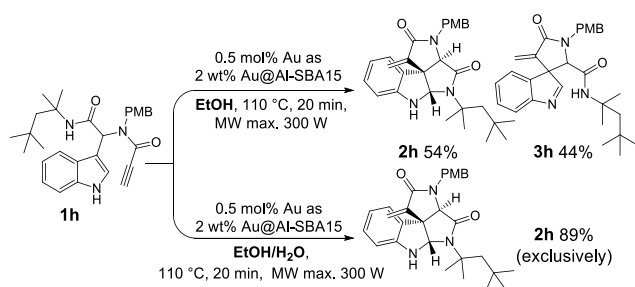


| | | | |
|---------------------------|---------------------------|---------------------------|---------------------------|
| | | | |
| (±)-2a 87% | (±)-2b 85% | (±)-2c 83% | (±)-2d 52% ^[a] |
| | | | |
| (±)-2e 80% | (±)-2f 80% ^[a] | (±)-2g 94% | (±)-2h 62% |
| | | | |
| (±)-2i 75% | (±)-2j 79% ^[a] | (±)-2k 80% ^[a] | (±)-2l 76% |
| | | | |
| (±)-2m 79% ^[a] | | | |

^{a)} Flow 10 μl/min; PMB = *para*-methoxybenzyl; PMP = *para*-methoxyphenyl.

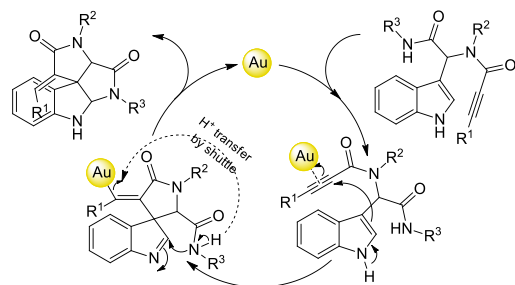
Several aliphatic (**2a** – **2f**, **2h**, **2i** and **2m**) and aromatic (**2g**, **2j** and **2k**) substituents in R¹-position were introduced providing spiroindolines in good to excellent yields (52 – 94 %). The unsubstituted alkyne **1l** was converted to the corresponding spiroindoline in good yield with 76 %. Variation in the R²-position tolerated the introduction of *p*-methoxybenzyl- (PMB; **2a**, **2c**, **2d**, **2h**, **2m**) and benzyl (**2g**, **2l**) protecting groups as well as various aliphatic (**2b**, **2e**, **2f**, **2i**, **2k**) substituents, such as butyl, cyclohexyl and isopropyl. The use of *tert*-butyl and cyclohexyl groups in R³-position provided similar yields, whereas the spiroindoline **2h** with a more sterically hindered alkyl group could be isolated in slightly lower yield.

To our delight, only a single isomer of **2h** could be detected in our continuous-flow experiments, whereas previous studies resulted into the isolation of an intermediate such as **3h** in Scheme 2.^[9] To further investigate the role of water in this matter, the reaction was performed with and without the addition of water in batch under microwave irradiation (MW), which can be seen in Scheme 2. We found that the presence of water results in an accelerated formation of spiroindoline **2h**.



Scheme 2. Study of the effect of water as additive in batch under microwave irradiation.

We hypothesize that a fast protodecoordination of the gold nanoparticle occurs in the presence of water, which is facilitated by a rapid proton transfer from the quaternary ammonium amide to the C–Au bond. The proposed mechanism for this reaction is shown in Scheme 3.



Scheme 3. Proposed mechanism for the Au NP-catalyzed cyclization and intra molecular trapping of the imine.

The reusability of the catalyst was investigated in batch as well as under flow conditions. In batch, no apparent loss in activity could be detected after 12 reaction cycles. However, under continuous-flow conditions the activity of the catalyst usually decreased

after eight injections of each 50 μmol. To determine the reason for the loss in activity ICP-OES, XPS and TEM measurements were conducted. It was suspected that the loss in activity is based on one of the following three scenarios: 1) leaching of the metal from the support, 2) change of the chemical composition of the catalyst, or 3) change of the crystal size.

Under microflow conditions, a leaching metal would be washed out of the reactor and thus the conversion rates would decrease over time.^[14] In other words, the catalyst bed functions as a catalyst reservoir which leaches gradually the catalytically active Au species into the reaction stream. Leaching of homogeneous gold species was investigated by ICP-OES measurements of the product mixtures and by analysis of fractionized samples of the used catalyst bed, which is shown in Table 3. The catalyst loading of the unused catalyst was determined to be 2.9 wt%. Table 2 shows no significant gold concentration gradient, thus leading to the assumption that no leaching occurs under our reaction conditions. This was supported by ICP-OES measurements of the reaction samples which showed no presence of any leached gold (< 90 ng/ml). Based on these results, leaching was excluded as a potential reason for the activity loss.

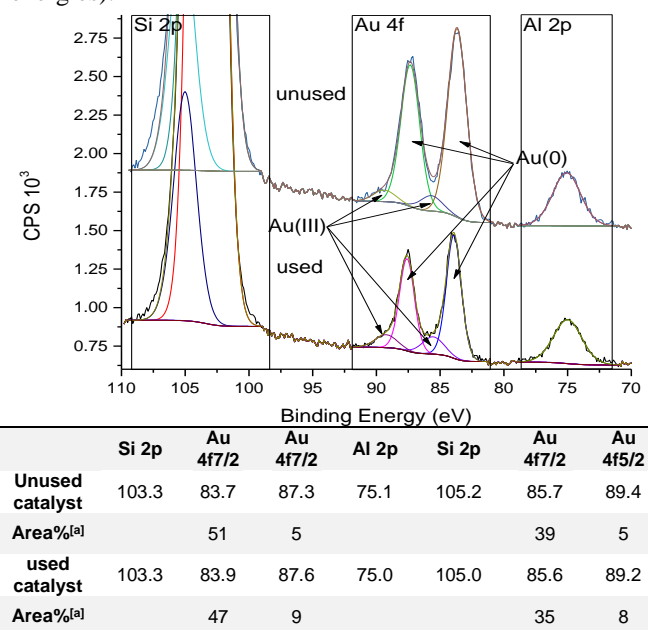
Table 3. Distribution of gold content in unused and used catalyst samples.

| unused catalyst [wt% Au] | used catalyst part 1 [wt% Au] | used catalyst part 2 [wt% Au] | used catalyst part 3 [wt% Au] |
|-----------------------------|----------------------------------|----------------------------------|----------------------------------|
| 2.87 | 2.85 | 2.9 | 2.93 |

Next, XPS measurements were carried out on samples of unused and used catalyst (Table 3). The results show the occurrence of Au_{4f} peaks (at 83.7 and 87.3 eV) in both samples, which proves the presence of 90 and 82 % Au(0) respectively. Furthermore, both samples indicate the presence of Au(III) as a small shoulder in the spectrum of the unused catalyst and a significant shoulder in the spectrum of the used catalyst (Au_{4f} peaks at 85.7 and 89.4 eV).^[15] The concentration of Au(0) seems to drop from 90 to 82 % during the reaction, whereas the Au(III) content rises from 10 to 17 %. When comparing the areas under the Al peaks with the combined areas under the Au(0) peaks and assuming the Al concentration in the samples is constant, it is obvious from the spectrum that the ratio between Au(0) and Al changed from the unused to the used catalyst sample. The ratios are Au/Al = 4.2/1 (unused) and Au/Al = 2.6/1 (used). Two reasonable explanations for the reduced activity can now be considered: The first is the formation of a significant Au(III) shoulder which would clearly indicate NP oxidation over time, thus possibly leading to the formation of an oxide layer on the surface and, therefore, to deactivation of the catalyst. The second is NP crystal growth which would reduce the available Au(0) surface in the sample, thus resulting in the reported ratio change between Au(0) and Al peaks.

The latter scenario is supported by two arguments: 1) A moderate shift of the Au_{4f} peaks in the XPS spectra, indicating a nanoparticle growth.^[16] 2) TEM images shown in Figures 1 and 2 which also indicate a crystal growth from finely dispersed NPs with a diameter between 1 and 5 nm to approx. 70 nm. Apparently, this vast increase in particle size exceeds a critical value, thus diminishing the catalytic activity of the nanoparticles over time.

Table 4. XPS spectra of the unused (top) and used (bottom) catalyst sample and results for XPS measurements (binding energies).



^{a)} Determined by absolute area integration.

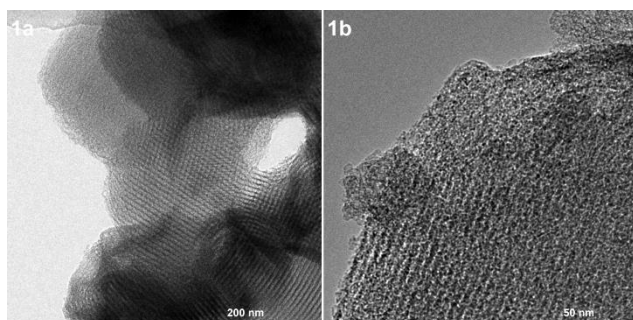


Figure 1. TEM images of the unused catalyst.

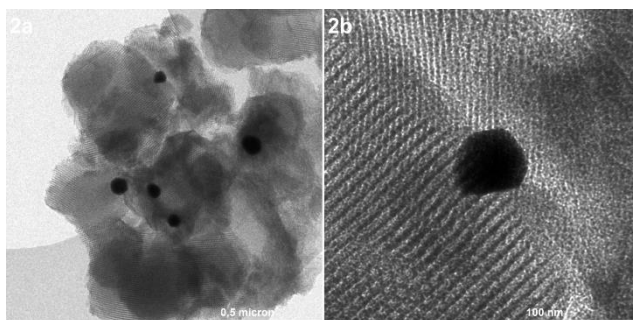


Figure 2. TEM images of the used catalyst showing distinct agglomerations of nanoparticles.

Conclusion

In summary, we have developed an efficient continuous-flow protocol for post-Ugi cycloisomerizations of complex structures with sterically hindered alkynes, using a heterogeneous Au@Al-SBA15 catalyst. Under microflow conditions good to excellent yields were obtained for substrates that showed little to no conversion under conventional batch conditions. The main reason for the conversion improvement is clearly the very high catalyst/reactant ratio in a packed bed reactor. Furthermore, the effect of water on the selectivity of the reaction was investigated. We hypothesize that the presence of water facilitates the protodecoordination of the gold nanoparticle and thus accelerates the overall catalytic process. In addition, catalyst deactivation was observed after prolonged use. No detectable leaching of the Au@Al-SBA15 catalytic bed was noted. However, our results show that deactivation of the catalyst species occurs via two alternative mechanisms: 1) oxidation of Au(0) to Au(III) and 2) agglomeration of the nanoparticles.

Experimental Section

Al-SBA15: The parent SBA-15 materials were prepared using tetraethylorthosilicate (TEOS) and aluminium isopropoxide. The triblock non-ionic copolymer EO20PO70EO20 (*Pluronic* P123 surfactant) was employed as template. The mesoporous material was prepared following a previously reported procedure.^[17] Under stirring *Pluronic* (8 g) was dissolved in HCl (300 mL) at pH 1.5. After 2 h of stirring at 40 °C and complete dissolution of the *Pluronic* the precursors were added in order to achieve a 20/1 ratio of Si/Al. Then the mixture was stirred for 24 h at 35 °C. Subsequently the mixture was subjected to a hydrothermal treatment at 100 °C for 24 h. The obtained white solid was filtered and oven-dried at 60 °C. The template was removed by calcination at 600 °C for 8 h, of which 4 h under N₂ and 4 h under air.

2%Au@Al-SBA15: Al-SBA15 (1 g) and HAuCl₄·3H₂O (0.0415 g) (equivalent to a theoretical 2 wt% Au) were milled together in a Retsch PM-100 planetary ball mill using a 125 mL reaction chamber and eighteen 10 mm stainless steel balls. Optimized milling conditions consisting of 10 min milling at 350 rpm were applied.^[18] Upon incorporation of the metal, the sample was calcined at 400 °C for 4 h under air.

Spiroindoline 2a: The substrate was placed into a test tube (50 μmol) and dissolved in a mixture of EtOH and water (500:1, 0.8 ml). The solution was injected into a 1 ml sample loop and 0.1 ml of the solvent mixture was used to transfer the complete sample volume into the sample loop. The reactor was equilibrated to a temperature of 120 °C and a pressure of ca. 10 bar. The sample was injected into the reactor with a flow of 15 μl/min. The product mixture was collected in a test tube. The run was considered to be complete when spotting the product solution on a TLC plate gave no visible spot anymore for the starting material. Next, the solvent was evaporated under reduced pressure to give the crude product which was subjected to silica gel chromatography (DCM/Et₂O = 10/1). After chromatography, last residues of solvents were removed by co-distillation with pentane (3x1 ml).

The reactor was used until a clear conversion drop was visible by TLC. In this case, the reactor was emptied,

cleaned and filled with fresh catalyst. On average, one reactor filling was used for up to 8 reactions.

Acknowledgements

FS is grateful to the “Agency for Innovation by Science and Technology” (IWT) for providing a PhD-scholarship. We acknowledge CatchBio for a postdoctoral fellowship to NE.

References

- [1] a) S. P. Nolan, *Acc. Chem. Res.* **2011**, *44*, 91-100; b) C. M. Friend, A. S. K. Hashmi, *Acc. Chem. Res.* **2014**, *47*, 729-730; c) A. Wittstock, M. Bäumer, *Acc. Chem. Res.* **2014**, *47*, 731-739; d) A. S. K. Hashmi, *Acc. Chem. Res.* **2014**, *47*, 864-876; e) Y.-M. Wang, A. D. Lackner, F. D. Toste, *Acc. Chem. Res.* **2014**, *47*, 889-901; f) C. Obradors, A. M. Echavarren, *Acc. Chem. Res.* **2014**, *47*, 902-912; g) B. Alcaide, P. Almendros, *Acc. Chem. Res.* **2014**, *47*, 939-952; h) L. Fensterbank, M. Malacria, *Acc. Chem. Res.* **2014**, *47*, 953-965.
- [2] a) A. Kumar, Z. Li, S. K. Sharma, V. S. Parmar, E. V. Van der Eycken, *Chem. Commun.* **2013**, *49*, 6803-6805; b) D. D. Vachhani, M. Galli, J. Jacobs, L. Van Meervelt, E. V. Van der Eycken, *Chem. Commun.* **2013**, *49*, 7171-7173; c) A. Kumar, Z. Li, S. K. Sharma, V. S. Parmar, E. V. Van der Eycken, *Org. Lett.* **2013**, *15*, 1874-1877.
- [3] a) R. Munirathinam, J. Huskens, W. Verboom, *Adv. Synth. Catal.* **2015**, *357*, 1093-1123; b) E. Shahbazali, V. Hessel, T. Noël, Q. Wang, in *Nanotechnol. Rev.*, Vol. 3, **2014**, p. 65; c) S. Liang, J. Jasinski, G. B. Hammond, B. Xu, *Org. Lett.* **2015**, *17*, 162-165; d) E. Gross, X.-Z. Shu, S. Alayoglu, H. A. Bechtel, M. C. Martin, F. D. Toste, G. A. Somorjai, *J. Am. Chem. Soc.* **2014**, *136*, 3624-3629; e) C. Lothschütz, J. Szlachetko, J. A. van Bokhoven, *ChemCatChem* **2014**, *6*, 443-448; f) E. Gross, H.-C. LiuJack, F. D. Toste, G. A. Somorjai, *Nat. Chem.* **2012**, *4*, 947-952; g) W. Huang, J. H.-C. Liu, P. Alayoglu, Y. Li, C. A. Witham, C.-K. Tsung, F. D. Toste, G. A. Somorjai, *J. Am. Chem. Soc.* **2010**, *132*, 16771-16773; h) L. Abahmane, J. M. Köhler, G. A. Groß, *Chem. Eur. J.* **2011**, *17*, 3005-3010.
- [4] a) F. Schröder, C. Tugny, E. Salanouve, H. Clavier, L. Giordano, D. Moraleda, Y. Gimbert, V. Mouriès-Mansuy, J.-P. Goddard, L. Fensterbank, *Organometallics* **2014**, *33*, 4051-4056; b) M. García-Mota, N. Cabello, F. Maseras, A. M. Echavarren, J. Pérez-Ramírez, N. Lopez, *ChemPhysChem* **2008**, *9*, 1624-1629; c) D. Tang, Z. Chen, J. Zhang, Y. Tang, Z. Xu, *Organometallics* **2014**, *33*, 6633-6642; d) C. Gryparis, C. Efe, C. Raptis, I. N. Lykakis, M. Stratakis, *Org. Lett.* **2012**, *14*, 2956-2959.
- [5] A. Homs, I. Escofet, A. M. Echavarren, *Org. Lett.* **2013**, *15*, 5782-5785.
- [6] A. Gunther, K. F. Jensen, *Lab on a Chip* **2006**, *6*, 1487-1503.
- [7] a) T. Noël, T. J. Maimone, S. L. Buchwald, *Angew. Chem., Int. Ed.* **2011**, *50*, 8900-8903; b) D. Scholz, C. Aellig, I. Hermans, *ChemSusChem* **2014**, *7*, 268-275.
- [8] I. Vural Gursel, T. Noël, Q. Wang, V. Hessel, *Green Chem.* **2015**, *17*, 2012-2026.
- [9] F. Schröder, M. Ojeda, N. Erdmann, J. Jacobs, R. Luque, T. Noel, L. Van Meervelt, J. Van der Eycken, E. V. Van der Eycken, *Green Chem.* **2015**, *17*, 3314-3318.
- [10] S. G. Modha, A. Kumar, D. D. Vachhani, J. Jacobs, S. K. Sharma, V. S. Parmar, L. Van Meervelt, E. V. Van der Eycken, *Angew. Chem. Int. Ed.* **2012**, *51*, 9572-9575.
- [11] a) M. Al-Naji, A. M. Balu, A. Roibu, M. Goepel, W.-D. Einicke, R. Luque, R. Glaser, *Catalysis Science & Technology* **2015**; b) M. Ojeda, A. M. Balu, V. Barron, A. Pineda, A. G. Coletto, A. A. Romero, R. Luque, *Journal of Materials Chemistry A* **2014**, *2*, 387-393; c) M. Ojeda, A. Pineda, A. A. Romero, V. Barrón, R. Luque, *ChemSusChem* **2014**, *7*, 1876-1880.
- [12] a) I. Denčić, S. de Vaan, T. Noël, J. Meuldijk, M. de Croon, V. Hessel, *Industrial & Engineering Chemistry Research* **2013**, *52*, 10951-10960; b) B. Tidona, S. Desportes, M. Altheimer, K. Ninck, P. R. von Rohr, *International Journal of Heat and Mass Transfer* **2012**, *55*, 522-530.
- [13] a) T. Noël, A. J. Musacchio, *Org. Lett.* **2011**, *13*, 5180-5183; b) T. Noël, S. Kuhn, A. J. Musacchio, K. F. Jensen, S. L. Buchwald, *Angew. Chem., Int. Ed.* **2011**, *50*, 5943-5946.
- [14] D. Cantillo, C. O. Kappe, *ChemCatChem* **2014**, *6*, 3286-3305.
- [15] NIST X-ray Photoelectron Spectroscopy Database, Version 4.1 (National Institute of Standards and Technology, Gaithersburg, 2012); <http://srdata.nist.gov/xps/>
- [16] a) F.-W. Chang, H.-Y. Yu, L. Selva Roselin, H.-C. Yang, *Applied Catalysis A: General* **2005**, *290*, 138-147; b) P. Konova, A. Naydenov, C. Venkov, D. Mehandjiev, D. Andreeva, T. Tabakova, *J. Mol. Catal. A: Chem.* **2004**, *213*, 235-240; c) M. Sankar, Q. He, M. Morad, J. Pritchard, S. J. Freakley, J. K. Edwards, S. H. Taylor, D. J. Morgan, A. F. Carley, D. W. Knight, C. J. Kiely, G. J. Hutchings, *ACS Nano* **2012**, *6*, 6600-6613.
- [17] A. Pineda, A. M. Balu, J. M. Campelo, R. Luque, A. A. Romero, J. C. Serrano-Ruiz, *Catal. Today* **2012**, *187*, 65-69.
- [18] A. Pineda, A. M. Balu, J. M. Campelo, A. A. Romero, D. Carmona, F. Balas, J. Santamaria, R. Luque, *ChemSusChem* **2011**, *4*, 1561-1565.

Leaching-Free Supported Gold Nanoparticles
catalyzing Cycloisomerizations under Microflow
Conditions

Adv. Synth. Catal. **Year**, *Volume*, Page – Page

Felix Schröder, Nico Erdmann, Timothy Noël,
Rafael Luque, Erik V. Van der Eycken*

